Id.: CR64

SIMULATION USING THE MONTE CARLO METHOD FOR THE SMEAR/FIELD FILTER COUNTER WITH POINT SOURCES

Fernando S. Santos[1], Ana B. C. Andrade[1], Davi S. Azevedo[1], Laila F. M. Almeida[1], Sara S. V. S. Lima[1], Bruno M. Mendes[1]

[1]Centro de Desenvolvimento de Tecnologia Nuclear – CDTN/CNEN – Universidade Federal de Minas Gerais – UFMG - Avenida Presidente Antônio Carlos, 6627, Pampulha, Belo Horizonte, MG, Brasil

fernando.soares@cdtn.br ; ana.andrade@cdtn.br ; davi.azevedo@cdtn.br ; laila.almeida@cdtn.br; sara.lima@cdtn.br ; bmm@cdtn.br

Palavras chaves: Monte Carlo Simulation; PHITS; Smear Counter/Field Filter.

ABSTRACT

Introduction: The Smear/Field Filter Counter is a device used for detecting and measuring radioactive contamination on surfaces, commonly found in radiation laboratories and nuclear facilities. The sensitive region of the counter consists of a sodium iodide crystal activated with thallium (NaI(Tl)). To enhance its performance and better understand its operation, computational simulation methods, such as Monte Carlo, are often employed to model the behavior of radioactive particles within the counter. **Objective:** This study aims to model and validate a Smear/Field Filter Counter using the Particle and Heavy Ion Transport Code System (PHITS). The simulated data were evaluated by comparison with experimental data acquired using Cesium-137 and Barium-133 point sources. **Methodology:** The geometries of the counter components were modeled in the PHITS code, including a 2 x 2" NaI(Tl) detector and the counter's shielding. The densities and chemical compositions of the modeled materials were obtained from the literature. The PHITS simulation also considered the distribution of channels in the real detector. Four different scenarios were simulated, each containing a type of point source, either Cs-137 (from three different models) or Ba-133 inside the counting chamber. Each simulated case resulted in a spectrum from the modeled detector using the t-deposit tally. The number of counts in the photopeak channel per photon emitted from the source corresponds to the system's absolute efficiency for the photopeak energy. A sufficient number of histories was simulated to obtain a statistical error of less than five percent. Validation with experimental data involved the same sources, in the same geometry, with each being counted three times for 6 minutes. The simulated and experimental absolute efficiencies were compared. **Results:** The simulated efficiency ranged from 4.4% to 5.2% for the Cs-137 sources (662 keV) and was 9.7% for the Ba-133 source (356 keV). Experimentally, efficiencies ranged from 4.5% to 4.6% for the Cs-137 sources and 9.2% for the Ba-133 source. Differences between the experimental and simulated values ranged from 3.5% to 11.3%, depending on the evaluated source. **Conclusions:** The smear counter was modeled in the PHITS code. The simulations showed comparable results with the experimental data, with differences ranging from 3.5% to 11.3%. Accuracy in modeling the sources and the distance between the source and the detector are crucial for the fidelity of the simulation results relative to the experimental values.

1. INTRODUCTION

The "Smear/Field Filter Counter" is a device used to detect and measure radioactive contamination on samples collected from surfaces or to count radioactive sources. This equipment is frequently employed in radiation protection to assess environments at risk of contamination with radioactive materials, such as nuclear facilities, radiation installations, research laboratories, hospitals, and clinics using radiopharmaceuticals for treatments and diagnostics, and industries handling open sources [1].

The sensitive region of the smear counter is typically composed of a scintillator capable of absorbing the incident radiation and emitting low-energy photons in the visible spectrum. One of the most commonly used scintillation materials is thallium-doped sodium iodide crystal, NaI(Tl). It is used due to its excellent radiation response characteristics, ease of production in large sizes, and ability to emit visible light proportional to the energy of the incident radiation. Additionally, NaI(Tl) has a linear response to photons across a wide range of energies [2,3].

The operating principle of this detector involves the excitation of valence band electrons by the incident radiation. These electrons, upon receiving sufficient energy, occupy energy levels created by the presence of the activator (thallium). When the electrons lose energy and return to the valence levels, they emit energy corresponding to the difference in levels in the form of photons, which propagate through the crystal structure. These photons are detected and converted into an electrical signal, which is subsequently processed to quantify the radioactivity present in the sample [2,4].

Monte Carlo simulations with scintillators can be performed and validated using experimental data, as done by Tam et al. (2017) in their study, where a Monte Carlo model of the NaI(Tl) detector was optimized using the Geant4 code. Various Monte Carlo codes have been used in this type of simulation, including PHITS (Particle and Heavy Ion Transport Code System). This code was developed through an international collaboration led by the Japan Atomic Energy Agency (JAEA), standing out as a robust and free tool compatible with Windows, capable of simulating a wide range of applications in nuclear physics, particle physics, medicine, radiation engineering, and radiation protection [5,6].

The objective of this study was to model and validate a Smear/Field Filter Counter using the PHITS code, version 3.341. The absolute efficiency data obtained in the simulations were evaluated by comparison with experimental data acquired with Cesium-137 and Barium-133 point sources.

2. METHODOLOGY

The Smear/Field Filter Counter is composed of two main parts: the counter shielding and the coupled scintillation detector. In Fig. 1A, a real image of the counter and a diagram with the actual dimensions of its respective parts (Fig. 1B) can be observed.

The detector used is a scintillation detector, CANBERA model 802, with NaI(Tl) scintillator crystal dimensions of 2” x 2”. The energy resolution (FWHM) is 9.0% for the Cs-137 peak [5]. In the crystal modeling, thallium doping was not considered, as libraries for this element are not included in the PHITS database, and it is assumed that its low concentration in the crystal should not significantly alter the interaction of radiation with the detector. The part of the detector located behind the crystal, not significantly influencing the detector counts, was simulated in a simplified manner. A glass plate (SiO_2) with a density of 2.2 g/cm³ was added to consider the backscatter in the photomultiplier tube components and other structures situated after the crystal [5].

The counter shielding is composed of three parts, as shown in Figure 1: the lead base, the truncated lead cone, and the stainless-steel counting chamber drawer. The truncated cone is covered by a stainless-steel tube. A PLA plastic tube was 3D printed to improve the fit of the detector into the truncated cone.

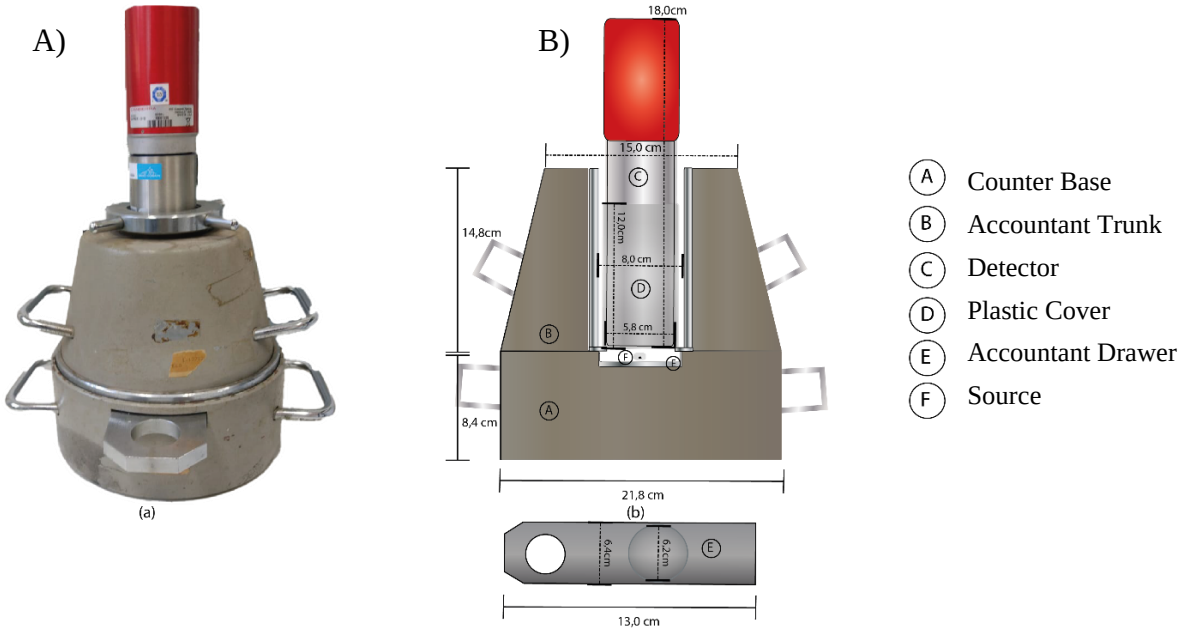

Fig. 1 - Smear Counter. A) Photo of the counting system. B) Diagram of the counter with its actual dimensions.

Tab. 1 - Atomic compositions and material densities.

Material	Density (g/cm³)	Composition	Weight Fractions
Lead	11.34	Pb	Pb: 1.000000
Steel 304	8.03	C Mn P S Si Cr Ni Fe	C: 0.000800 Mn: 0.020000 P: 0.000450 S: 0.000300 Si: 0.010000 Cr: 0.190000 Ni: 0.095000 Fe: 0.683450
Argon	0.001205	C N O Ar	C: 0.000124 N: 0.755268 O: 0.231781 Ar: 0.012827
Sodium Iodide	3.67	Na I	Na: 0.152956 I: 0.844324
Aluminum	2.70	Al	Al: 1.000000
Silicon Dioxide	2.65	Si O	Si: 0.467000 O: 0.533000
PLA Plastic	1.21	C H O	C: 0.500000 H: 0.055000 O: 0.445000
Detector Window	2.94	Al	Al: 1.000000
Source Acrylic	1.19	C H O	C: 0.599836 H: 0.080545 O: 0.319619

The density and chemical composition of the materials used in the simulations were obtained from the Compendium of Material Composition Data for Radiation Transport Modeling [7] and are presented in Table 1.

Three source models were developed to validate the simulation, totaling four different sources: three Cs-137 sources and one Ba-133 source. We considered only the 356 keV peak because it is clearly identifiable in the spectra and it had the highest probability of emission. The only difference between each model is the geometry and materials of the source type. Model I was the same for a Cs-137 source and a Ba-133 source. The sources are centralized, enclosed in an acrylic cylinder. A photograph of these sources can be seen in Fig. 2A. In Fig. 2B, a schematic representation of this source model with its dimensions used in the simulations is shown.

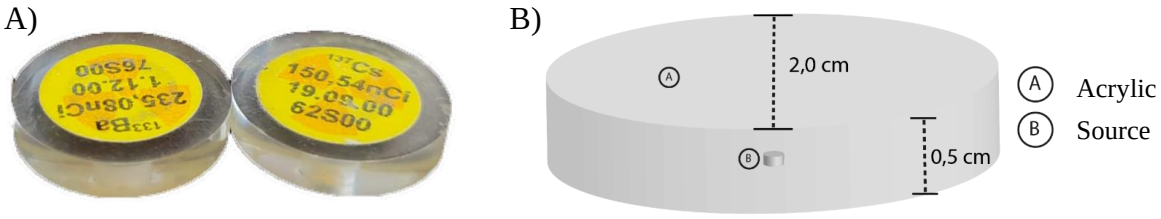

Fig. 2 - Sources of Cs-137 and Ba-133 from model I. A) Photograph of the sources. B) Schematic representation of the sources demonstrating the dimensions used in the simulations.

Model II is a Cs-137 source. The source is centralized, encased in an aluminum base, and the surface has a thin layer of Mylar, added to uniformize the radiation emission. A photo of the source can be seen in Fig. 3A, and Fig. 3B shows a detailed schematic with the respective measurements. In the simulations with this source, the Mylar and polyamide film were not considered. The other structures were modeled.

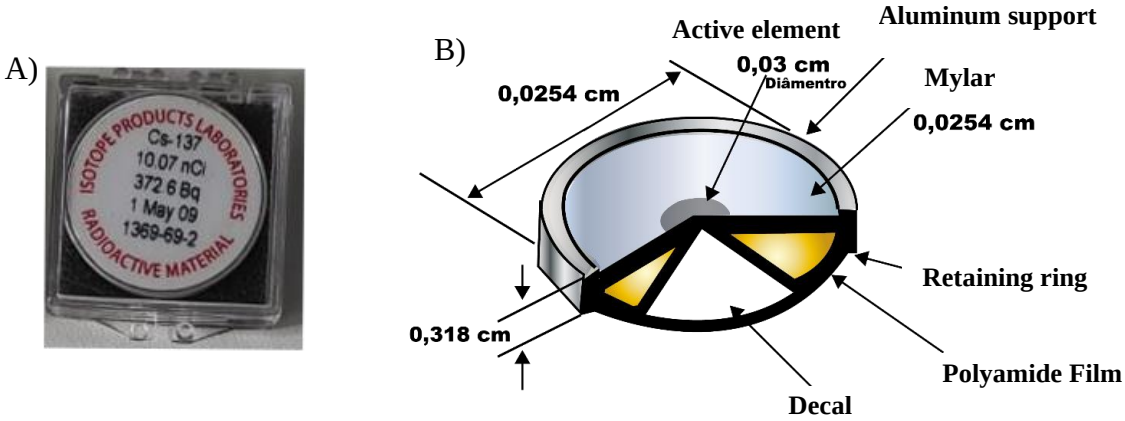

Fig. 3 - Demonstration of Model II Source. A) Photograph of the source. B) Schematic representation of the source showing the dimensions used in the simulations (adapted from the manufacturer).

The Cs-137 source in Model III (Fig. 4A) has a geometry similar to that of Model II. An experiment using radiochromic film was conducted to determine the shape and position of the active element (Fig. 4B). The impression formed on the radiochromic film showed that the active

element is not centered within the aluminum piece; this deviation was also considered in the simulation. Fig. 4C presents a schematic with the dimensions of the Model III source.

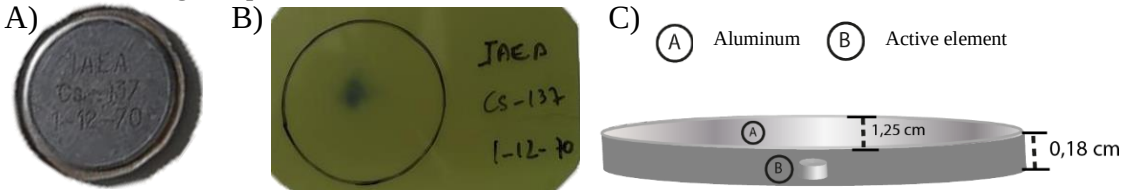

Fig. 4 – Cs-137 Source in Model III. A) Photograph of the source. B) Position and shape of the active element of the source evaluated with radiochromic film. C) Schematic indicating the dimensions of the source used in the simulations.

The simulations were performed using the PHITS code, version 3.31. Standard libraries were employed. In each case, 10^6 particle histories were simulated. The tally t-deposit was used to determine the number of particle counts as a function of the energy deposited in the detector's crystal per particle emitted by the source. The energy ranges for detecting the counts were determined to replicate the configurations applied to the NaI(Tl) detector. Thus, 1024 energy channels were configured, ranging from 0 to 3072 keV, with increments of 3 keV each.

The GENIE 2000 software was used for acquiring experimental data. It is a program for the analysis of radiation spectra. GENIE 2000 can process and analyze gamma spectra, providing detailed information on the energies and intensities of the detected radiations. The acquisitions were performed with a time of 360 s. Three measurements were taken for each source. The mean and standard deviation were calculated to evaluate the statistical errors of the measurements. The experimental efficiency was calculated as the ratio between the area of the photopeak of interest in the gamma spectrum and the total number of photons emitted by the source during the counting time.

3. RESULTS

The computational model of the smear counter was executed and can be observed in Fig. 5. The sources from models I, II, and III can also be visualized in the figure. The simplification of the detector's posterior part is shown in green.

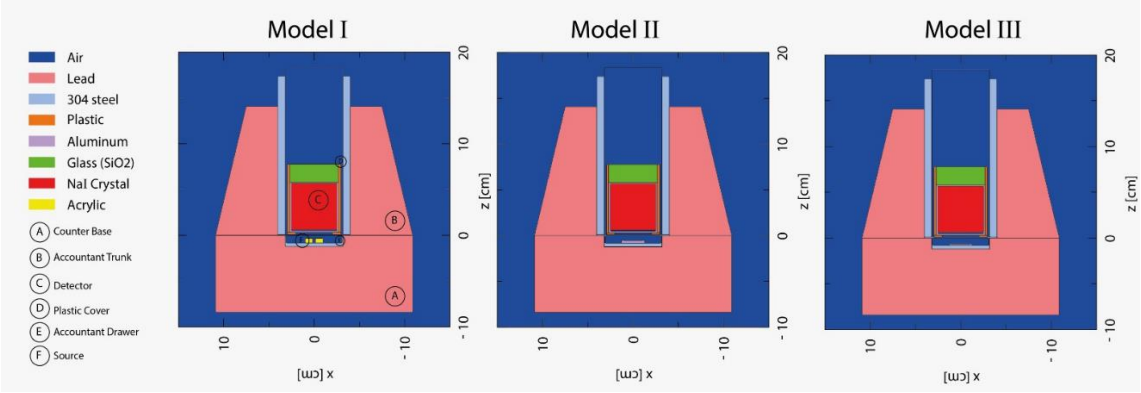

Fig. *5* - Computational model of the counter and its adaptations for each source model.

The experimental and simulated spectra obtained for the Cs-137 and Ba-133 sources from model I were presented in Fig. 6. It can be observed that the simulations do not account for the detector's energy resolution. Thus, the photopeaks are generated only in the channel corresponding to the energy of the photon emitted by the source. It can also be noted that, in the case of Ba-133, only 356 keV photons were generated in the simulated cases. This energy corresponds to the photon with the highest probability of emission from Ba-133 in that region of the spectrum. Small peaks from the 303 keV and 384 keV photons, with a low probability of emission, can also be observed in Fig. 6D.

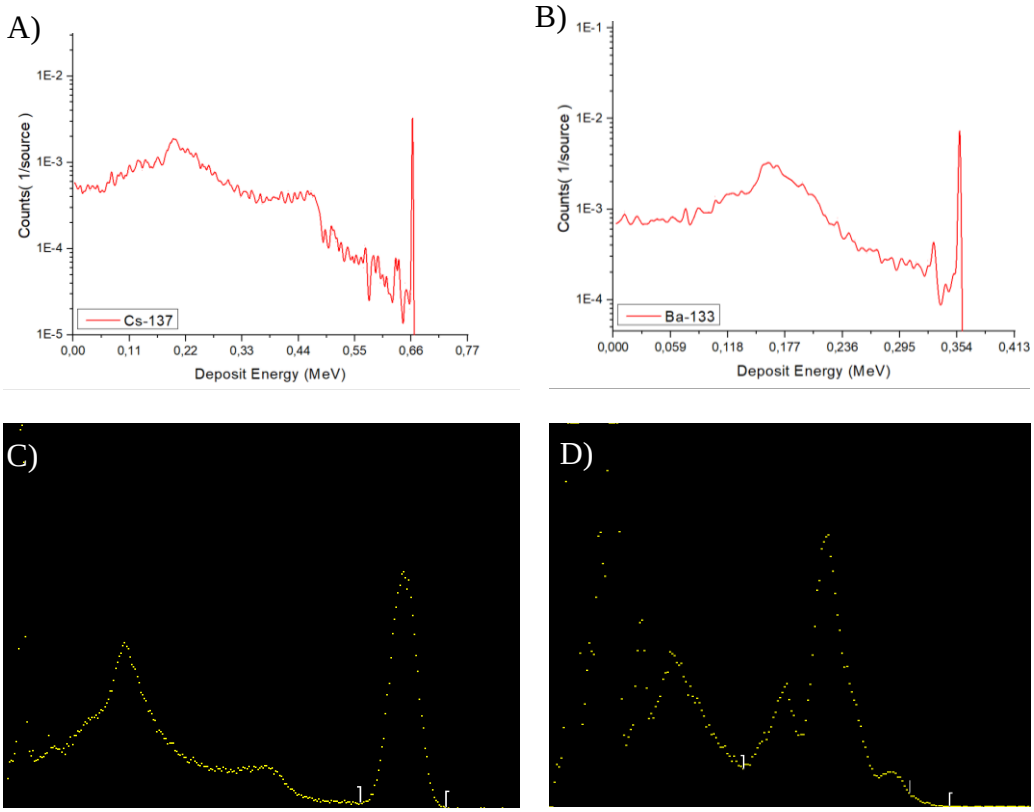

Fig. 6 - Spectra of the Cs-137 and Ba-133 sources from Model I. Simulated spectra of Cs-137 (A) and Ba-133 (B). Experimental spectra of Cs-137 (C) and Ba-133 (D).

Table 2 shows a comparison between experimentally and simulated efficiencies. The smallest differences were observed for sources from Model I. The modeling of these sources was facilitated because they are made of transparent acrylic, which explains the smaller variations obtained for Ba-133 and Cs-137 sources from this model.

Tab. 2 - Comparison between efficiency obtained from experimental and simulated data.

Models	**Source**	**Activity (nCi)**	**Emission Peak (MeV)**	**Experimental Efficiency**	**Simulated Efficiency**	**Difference**
Model I	Cs-137	87.65	0.6617	4.6 % ± 0.06	4.44 % ± 0.01	3.5 %
	Ba-133	49.88	0.3560	9.16 % ± 0.03	9.70 % ± 0.01	5.9 %
Model II	Cs-137	7.11	0.6617	4.58 % ± 0.004	5.16 % ± 0.07	11.3 %
Model III	Cs-137	2981.82	0.6617	4.46 % ± 0.02	4.96 % ± 0.01	10.1 %

The sources from Models II and III showed differences of approximately 10% between the simulated and experimental values. These variations can be attributed to geometric characteristics of the sources that were not accurately represented in the simulations. For the Cs-137 source from Model III, it was observed that the source was not centered (Fig. 4B), and the exact dimensions, as well as the distribution of activity in the active area, could not be determined. In Model II, although several dimensions were provided by the manufacturer, the height and thickness of the active element were unclear. Additionally, the model generated in the simulation was more simplistic than the actual one. Thus, the modeling inaccuracies may have contributed to the differences observed between the experimental and computational results.

Furthermore, true coincidence effects, could occur when photons emitted in almost simultaneously decays are detected as a single event. In this case, they may be recorded as a sum of their energies, resulting in peaks that do not represent the individual energies of the photons. That effect may have impacted the experimental efficiency of Ba-133 source, which also emits photons of 81 keV and 276 keV. These photons, when detected in coincidence, could affect the 356 keV peak.

The presence of these true coincidence peaks may slightly increase the experimental efficiency of the peak of 356 keV of Ba-133, as the detector may record false events with the sum of the 81 keV and 276 keV energies in the 356 keV photopeak. However, the source activity is very low. The dead time was lower than 1%. So, we believe the influence of the true coincidence effects could be considered negligible in this case.

4. CONCLUSION

The Monte Carlo code PHITS was used to simulate photon transport from Cs-137 and Ba-133 sources in a swipe counter model, and the results obtained from the simulation were compared with experimental results.

The counting efficiency results showed differences ranging from 3.5% to 11.3% between simulated and experimental values. The source models that presented the greatest difficulty for detailed simulation were those with the largest differences.

It was possible to determine that a crucial point in this type of simulation is the precision in defining the source, both in terms of its geometric characteristics and emission properties. Small variations, such as height and positioning, can result in significant changes in simulated efficiency. Additionally, the distance between the source and the detector was another parameter that could result in large discrepancies between simulated and experimental results. Therefore, simulating models of sources different from those already modeled will require new definitions of geometry and source to ensure greater fidelity of results.

Future work will focus on better modeling of sources from Models II and III and validating the swipe counter model for sources with energy emissions above and below those already researched.

5. ACKNOWLEDGMENTS

The following Brazilian institutions support this research project: Center for Development of Nuclear Technology (CDTN), National Council for Scientific and Technological Development (CNPq), and Coordination for the Improvement of Higher Education Personnel (CAPES). This work is also part of INCT/INAIS, CNPq project 406303/2022-3.

BIBLIOGRAPHIC REFERENCES

[1] https://www.mirion.com/products/technologies/health-physics-radiation-safety-instruments/portable-radiation-measurement/handheld-health-physics-instruments/easy-count-field-smear-filter-counter acessado em 24/06/2024.

[2] L. Tauhata *et al.*, Radioproteção e Dosimetria: Fundamentosb- 9ª revisão, IRD/CNEN, pp. 201-204, Rio de Janeiro (2013).

[3] S. Ashrafi *et al.*, Monte-Carlo modeling of a NaI (Tl) scintillator. Journal of radioanalytical and nuclear chemistry, v. 269, n. 1, p. 95-98 (2006).

[4] S. Boukhalfa *et al.*, Monte Carlo simulation of NaI (Tl) detector and GRAVEL deconvolution for biological, geological samples and their dosimetry evaluation. Journal of Instrumentation, v. 16, n. 09, p. P09024 (2021).

[5] H. D. Tam *et al.*, Optimization of the Monte Carlo simulation model of NaI (Tl) detector by Geant4 code. Applied Radiation and Isotopes, v. 130, p. 75-79 (2017).

[6] Japan Atomic Energy Agency. PHITS: Particle and Heavy Ion Transport code System, version 3.341. Tokai-mura, Japan: Japan Atomic Energy Agency, Software (2023).

[7] R. S. Detwiler *et al*. Compendium of material composition data for radiation transport modeling. Pacific Northwest National Lab.(PNNL), Richland, WA (United States) (2021).